PALEOCEANOGRAPHY, VOL. 13, NO. 4, PAGES 384-394, AUGUST 1998

# New aspects of organic carbon deposition and its paleoceanographic implications along the northern Barents Sea margin during the last 30,000 years

Jochen Knies and Ruediger Stein

Alfred Wegener Institute for Polar and Marine Research, Bremerhaven, Germany

**Abstract.** We studied variations in terrigenous (TOM) and marine organic matter (MOM) input in a sediment core on the northern Barents Sea margin over the last 30 ka. Using a multiproxy approach, we reconstructed processes controlling organic carbon deposition and investigated their paleoceanographic significance in the North Atlantic-Arctic Gateways. Variations in paleo-surface-water productivity are not documented in amount and composition of organic carbon. The highest level of MOM was deposited during 25-23 ka as a result of scavenging on fine-grained, reworked, and TOM-rich material released by the retreating Svalbard/Barents Sea ice sheet during the late Weichselian. A second peak of MOM is preserved because of sorptive protection by detrital and terrigenous organic matter, higher surface-water productivity due to permanent intrusion of Atlantic water, and high suspension load release by melting sea ice during 15.9-11.2 ka.

## 1. Introduction

The Arctic's impact on the global climate system is significantly controlled by the inflow of Atlantic water masses [e.g., *Hebbeln and Wefer*, 1997]. Relatively warm Atlantic surface water passes through the Fram Strait and the Barents Sea into the Arctic Ocean and thus maintains poleward heat transport and water exchange with the Atlantic Ocean [e.g., *Blindheim*, 1989; *Rudels et al.*, 1994]. Additionally, Atlantic water inflow coupled with the marginal ice zone (MIZ) influences significantly the primary production rates in the Arctic Ocean [*Heimdal*, 1983; *Anderson*, 1995]. Recent investigations revealed that the Arctic Ocean is dynamically coupled to the Atlantic and is much (probably by a factor of 10) more productive than previously thought [*Macdonald*, 1996; *Wheeler et al.*, 1996]. Short-term Atlantic water advection to the western Svalbard margin and the Fram Strait that resulted in seasonally ice-free conditions with significantly enhanced primary production rates at the MIZ during the late Weichselian has also been reported [*Hebbeln et al.*, 1994; *Dokken and Hald*, 1996]. The enhanced bottom water formation due to brine release during seasonal sea ice formation enables the Arctic Ocean and its Atlantic-water-influenced seas to play an important role as a sink for atmospheric $CO_2$ [*Midttun*, 1985; *Broecker et al.*, 1990; *Quadfasel et al.*, 1988; *Boyle*, 1988; *Anderson and Jones*, 1991; *Anderson*, 1995].

In surface samples of the Arctic Ocean, minor amounts of marine organic matter (MOM) are preserved only in the vicinity of the Atlantic water inflow and in areas of seasonally open-water conditions [*Stein et al.*, 1994b; *Fahl and Stein*, 1997; *Schubert and Stein*, 1997]. Generally, the organic carbon in the Arctic Ocean sedimentary record is dominated by terrigenous organic matter (TOM). This TOM is entrained within the sea ice on the Eurasian shelves and released during ice drift in areas of extensive melting and/or transported by turbidites [*Stein et al.*, 1994a; *Schubert and Stein*, 1996]. However, for areas where Atlantic water submerges into the Arctic Ocean, little information about organic carbon deposition during the last glacial/interglacial cycle exists [*Thiede et al.*, 1996]. Therefore a comparison of marine and terrestrial biomarker distributions with more conventional sedimentological climate proxies from an exceptionally well dated Arctic Ocean sediment core may give new insights into the carbon cycle in this high-latitude area.

In this paper we use geochemical, sedimentological, and stable isotope data to decipher processes controlling organic carbon deposition and its paleoceanographic significance along the northern Barents Sea margin. The study compares biomarkers indicative for marine and terrigenous organic matter, respectively, with other climate proxies in order to show the importance of a multiproxy approach for paleoproductivity reconstructions of the northern Barents Sea margin over the last 30 kyr. Detailed investigations of the organic matter composition and its importance for interpretations in terms of surface-water productivity, preservation of MOM, and supply of TOM at the transitional zone of Atlantic to the Arctic Ocean are the major objectives of this work.

## 2. Material and Methods

During R/V *Polarstern* cruise Ark VIII/2 [*Rachor*, 1992], gravity core PS2138-1 (81°32.1 N, 30°35.6 E; 995 m water depth) was recovered on the northern continental slope of the Barents Sea (Figure 1). Selection of core position was based on high-resolution Parasound echosounding system (4 kHz). The sediments mainly consist of bioturbated mud, which is occasionally interrupted by laminated sequences and layers of sand and gravel (Figure 2).



Paper number 98PA01501.
0883-8305/98/98PA-01501$12.00

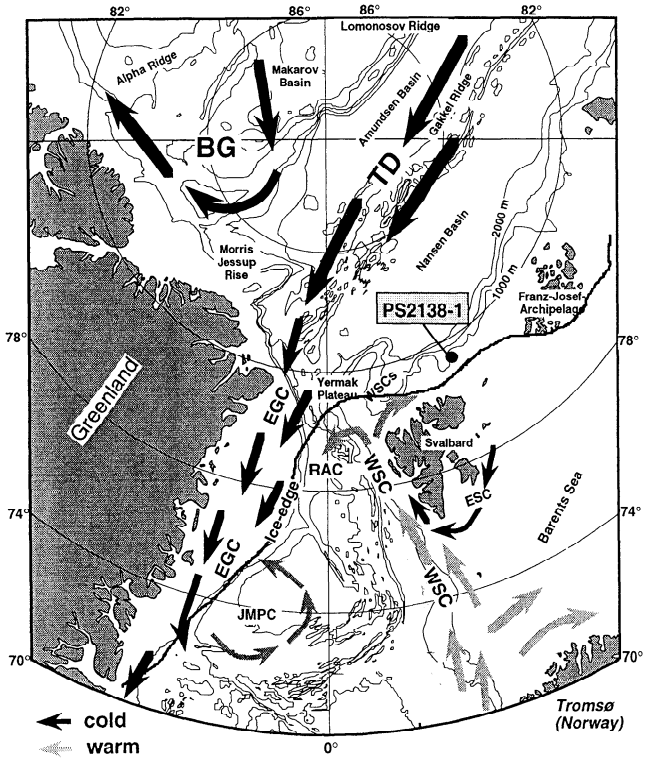


**Figure 1.** Surface currents and average summer ice conditions in the European sector of the Arctic Ocean [*Sudgen*, 1982]. Location of core PS2138-1 is indicated by the solid circle. Abbrevations are TPD, Transpolar drift; BG, Beaufort Gyre; EGC, East Greenland Current; WSC, West Spitsbergen Current; $WSC_s$, West Spitsbergen Current (submer-ging); ESC, East Spitsbergen Current; RAC, Return Atlantic Current; and JMPC, Jan Mayen Polar Current. A detailed description of the oceanographic setting in the study area is given by *Hebbeln and Wefer* [1997].

### 2.1. Sampling and Bulk Analysis

The core was routinely sampled at 5-10 cm intervals for sedimentological characteristics and lipid biomarkers; additional samples were taken in intervals of changing lithology and/or color. The characterization of lithology and structure was performed on X radiographs. Coarse-grained detritus >2 mm was counted in 1 cm intervals from the X radiographs to evaluate the content of ice-rafted debris (IRD) [*Grobe*, 1987]. To separate the sand and gravel fraction (>63 μm in wt. %) from the silt and clay fraction, each sample was rinsed through a 63 μm mesh. After drying for >48 hours at 50 °C, the coarse fraction was weighed. From the <63 μm fraction the silt and clay fractions were separated using settling tubes ("Atterberg method") [*Müller*, 1967].

Total carbon, nitrogen, and organic carbon contents were determined by means of a Heraeus CHN-O-RAPID elemental analyzer. The carbonate content was calculated as $CaCO_3$ (percent)= (TC-TOC)8.333, where TC (percent) is total carbon and TOC (percent) is total organic carbon [*Stein*, 1991, and references therein]. The carbon and nitrogen measurements have a standard deviation of 0.06% and 0.02%, respectively.

The dolomite content (percent) was determined by C. Vogt (unpublished data, 1997) by means of a Phillips PW 3020 diffractometer equipped with a cobalt kå radiation. Measurements were performed from 2° to 100° theta with a 0.02° theta step $s^{-1}$ mode. The minerals were determined using the Qualit software package [*Emmermann and Lauterjung*, 1990]. The precision of dolomite determination is ±1%. The amount of biogenic calcite was assumed by subtracting the dolomite from the carbonate content.

The hydrogen index (HI) was achieved by means of Rock-Eval pyrolysis as described by *Espitalié et al.* [1977]. The III-value corresponds to the quantity of pyrolyzable hydrocarbons per gram TOC (mg HC (g TOC)$^{-1}$). The reproducibility is ±8%. Biogenic silicate (percent) was measured by molybdate-blue spectrophotometry on dissolved ground bulk samples using an automated leaching technique [*Müller and Schneider*, 1993, and references therein]. The standard deviation of samples with different opal contents is –±5% [*Bonn*, 1995].

Mass accumulation rates (g $cm^{-2}$ $kyr^{-1}$) of bulk sediment ($AR_{bulk}$) were calculated from linear sedimentation rates (cm $kyr^{-1}$; based on calibrated ages) and dry bulk density data (g $cm^{-3}$) [*van Andel et al.*, 1975]. Dry bulk density was determined by weighing 5 $cm^3$ of dry sediment, measuring volume and density by Accupyc1330 (Micromeritices), and calculating wet bulk density and porosity according to *Gealy* [1971].

### 2.2. Mass Spectrometry Analysis

Stable carbon isotope ratios of the organic fraction were determined on decarbonated samples using a Finnigan MAT Delta-S mass spectrometer (AWI, Potsdam). Accuracy was checked by parallel analysis of international standard reference material (IAEA-CH-7). Results are expressed in the δ notation (permille versus Vienna Pee Dee Belemnite (PDB)). The analytical precision of the analysis is –±0.2‰. A Finnigan MAT 251 mass spectrometer (AWI, Bremerhaven) was used to perform stable oxygen and carbon isotope measurements on the planktonic foraminifera *Neogloboquadrina pachyderma* (sinistral (sin.)) from the >63 μm fraction. Results are expressed in the δ notation (permille versus PDB) and external reproducibility is 0.09‰ for $\delta^{18}O$ and 0.06‰ for $\delta^{13}C$ [*Mackensen et al.*, 1994]. Results are calibrated against the National Institute of Standards and Technology (NIST) 19 standards. Several samples were chosen for AMS $^{14}C$ dating (Kiel, University) (Table 1). The $^{14}C$ dates are $\delta^{13}C$-normalized and corrected for reservoir effects equal to 440 yr [*Mangerud and Gulliksen*, 1975]. The radiocarbon age was calibrated to a calendar age using the program Calib 3.0 [*Stuiver and Reimer*, 1993] for ages <18 $^{14}C$ ka and an extended second-order fit for the period >18 $^{14}C$ ka [*E. Bard et al.*, 1992].

### 2.3. Lipid Analysis

For the lipid extraction, –2-3 g of each sample was freeze-dried and treated with 10-15 mL methanol, methanol: dichloromethane (1:1), and dichloromethane. An internal standard (squalan) was added. The *n*-alkanes and long-chain unsaturated $C_{37}$ alkenones were separated from the other fractions by column chromatography with hexane and

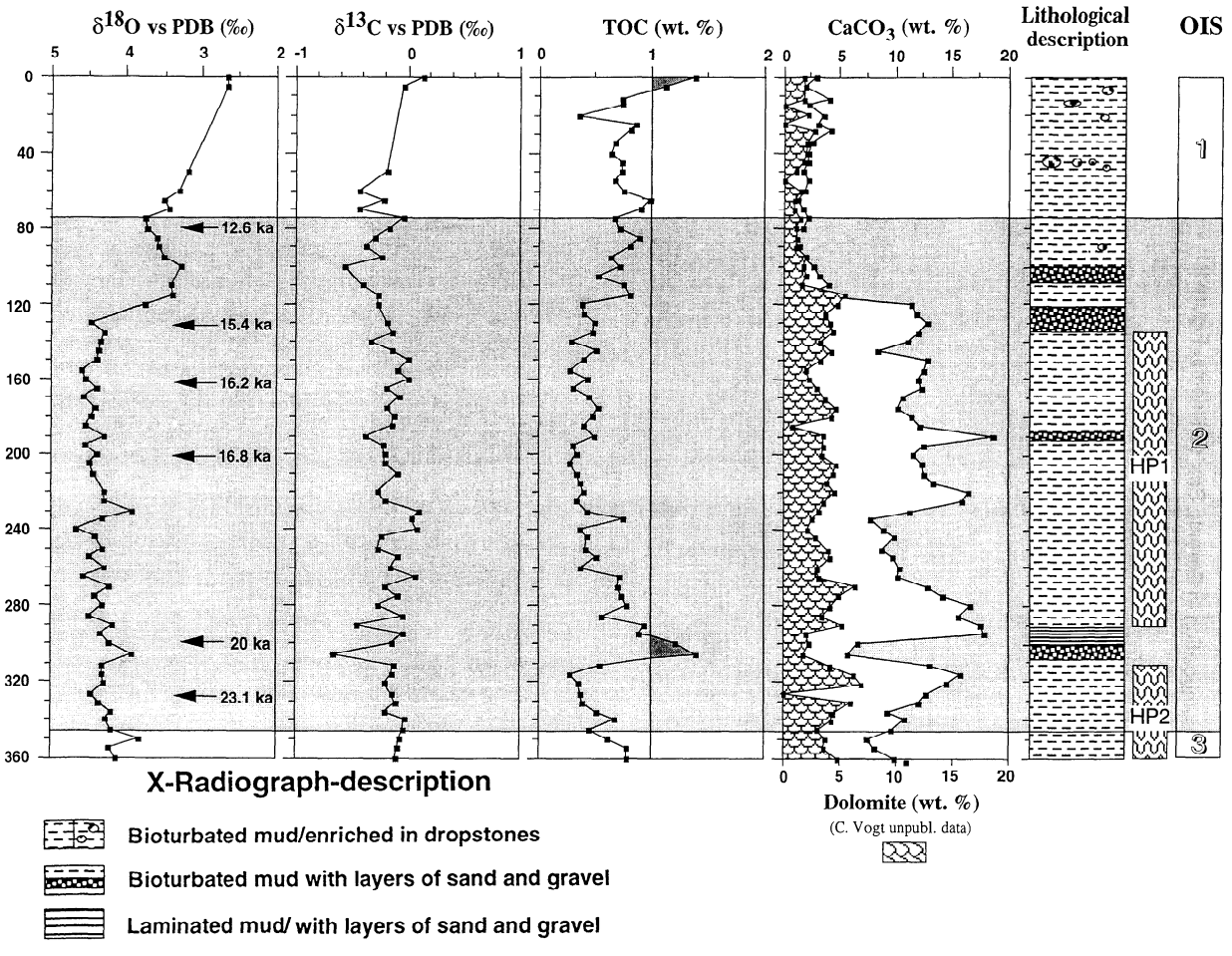


**Figure 2.** Compilation of stable oxygen and carbon isotope records (*Neogloboquadrina pachyderma* sin.), total organic carbon (wt. %), carbonate and dolomite content (wt. %), and lithological description of sediment core PS2138-1. Age control and stratigraphical framework are based on Accelerator Mass Spectrometry (AMS) $^{14}C$ dates, and oxygen isotope boundaries are after *Martinson et al.* [1987]. Oxygen isotope stages are displayed on the right. HP1 and 2, high productive zones, are defined according to *Hebbeln et al.* [1994] and *Dokken and Hald* [1996].

hexane:ethylacetate (97:3), respectively. The *n*-alkanes were analyzed using a Hewlett-Packard 5890 gas chromatograph (GC) fitted with a cold injection system by Gerstel and an ultra-1 fused silica capillary column ((50 m)(0.25); film thickness 0.25 μm). Helium was used as a carrier gas. Analyses were performed with the following sequence of oven temperature: 60°C (1 min), 150°C (rate: 10°C $min^{-1}$), 300 °C (rate: 4°C $min^{-1}$), and 300°C (45 min isothermal). The precision for the *n*-alkane analysis was better than ±10%. The fraction containing $C_{37}$ alkenones was saponified with 1 M potassium hydroxide in 95% methanol for 2 hours at 90°C. The following temperature program was used: 60°C (1 min), 270°C (rate 20°C $min^{-1}$), 320°C (1°C $min^{-1}$), and 320°C (20 min isothermal). Because of the low alkenone concentrations, results obtained by GC were checked by GC/MS technique. $C_{37}$ alkenones could not be quantified in the core. Very low concentrations in two samples are presented as relative abundances of the total extract.

Fatty acids were extracted in 15 mL dichloromethane:methanol 2:1 for 24 hours and spiked with an internal standard (fatty acid methyl ester 19:0). An aliquot of the total extract was transesterified for 4 hours at 80°C with 3% concentrated sulfuric acid in methanol. Four mL of Milli-Q were added, and the fatty acids were extracted three times in hexane. One μL of the extract was analysed using the GC with DB-FFAP as liquid phase. The oven temperature program for the fatty acids was as follows: 160°C, 240°C (rate: 4°C $min^{-1}$), 240°C (15 min isothermal) (modified according to *Kattner and Fricke* [1986]). The precision for the fatty acid analysis was better than ±12%. Data for *n*-alkanes and fatty acids were acquired, and peak areas were quantified automatically using a HP Chem-Station.

The abundance of chlorophyll-derived pigments was measured using a UVvis spectrophotometer by Kontron. The freeze-dried and homogenized samples are extracted in 90% acetone (25 mL). The total abundances of photosynthetic pigments (tetrapyrroles) were estimated by measuring the absorbance of the extracts in the Soret band (i.e., 410 nm). Maxima absorption in the Satellite band at 665 nm apart from the Soret band at 410 nm shows the presence of chlorin-like pigments in the sediments [*Rosell-Melé and Koç*, 1997; *Rosell-Melé et al.*, 1997]. The turbidity factor (absorbance at 750 nm) has been subtracted. The reproducibility of the measurements was better than ±7%.

**Table 1.** Results of Accelerator Mass Spectrometry (AMS) $^{14}C$ Datings, Corresponding Calendar Ages and Calculated Linear Sedimentation Rates (LSR) Deduced from the Stratigraphic Data

| Core | Depth in Core, cmbsf[a] | Material | Corrected Ages, $^{14}C$ years[b] | Calibrated Ages[c] | Laboratory reference Number | LSR (cmkyr$^{-1}$) |
|---|---|---|---|---|---|---|
| PS2138-1 | 80 | Bivalves | 12600+140/-130 | 14796 | KIA363 | 5.4 |
| PS2138-1 | 130 | mixed forams | 15410+130/-130 | 18325 | KIA1283 | 14.2 |
| PS2138-1 | 160 | *N. pachyderma* sin.[d] | 16230+210/-210 | 19111 | KIA364 | 37.9 |
| PS2138-1 | 200 | *N. pachyderma* sin. | 16880+130/-130 | 20573 | KIA2745 | 27.4 |
| PS2138-1 | 300 | *N. pachyderma* sin. | 20040+330/-320 | 24007 | KIA365 | 29.1 |
| PS2138-1 | 331 | *N. pachyderma* sin. | 23100+240/-240 | 27185 | KIA2744 | 9.7 |
| PS2138-1 | 345 | OIS2/3 boundary[e] | 24000 | 28200 | | 14.0 |

[a] Centimeters below the surface.

[b] A 440 ycar reservoir correction was applied to all ages.

[c] The radiocarbon ages for the period up to 18 $^{14}C$-years were calibrated to a calendar date using the program Calib 3.0 [*Stuiver and Reimer*, 1993; *Bard et al.*, 1993] and an extended second-order fit [*Bard et al.*, 1992] for the interval up to 30 $^{14}C$-years.

[d] *Neogloboquadrina pachyderma* sinistral.

[e] Oxygen isotope stage boundary 2/3. Age follows the timescale of *Martinson et al.* [1987].

## 3. Results

### 3.1. Age Model

The stratigraphic framework is based on oxygen isotope record of planktonic foraminifera *Neogloboquadrina pachyderma* (sin.) (Figure 2). The definition of oxygen isotope stages (OIS) and their conversion into absolute ages follow the timescale of *Martinson et al.* [1987]. The stratigraphical control is further modified by several radiocarbon (AMS$^{14}C$) datings (Table 1). The chronology was supplemented by carbon isotopes of *N. pachyderma* (sin.), the percent of organic carbon, and the carbonate content (Figure 2). During OIS 2, the heaviest $\delta^{18}O$ values (4‰-4.6‰) are observed. A prominent organic carbon peak dated between 22.5 and 19.5 $^{14}C$ kyr on the western Svalbard margin and the Fram Strait is clearly identified in the core (Figure 2) [*Hebbeln et al.*, 1994; *Elverhøi et al.*, 1995]. The OIS 2/3 boundary is indicated by a slight shift to lighter $\delta^{18}O$ and heavier $\delta^{13}C$ values. The beginning of the last deglaciation (Termination I) is dated at 15.4 $^{14}C$ ka and is well defined by increasing $\delta^{18}O$ values, decreasing $\delta^{13}C$ values, and a distinct input of coarse-grained material (Figure 2). The OIS 1/2 boundary is based on the measured AMS$^{14}C$ age. A general $\delta^{18}O$ decrease to Holocene levels is observed at 60 cm. The age control points were converted to calendar years and then linearly interpolated between these points to determine numerical ages for each sample, assuming uniform sedimentation rates (Table 1). When not specified as $^{14}C$ ages, given ages are calibrated calendar ages.

### 3.2. Terrigenous Signal

In the remainder of this paper, profiles of organic carbon composition, sedimentary proxies, and accumulation rates are plotted against calibrated ages. In order to compensate for dilution effects caused by variations in sedimentation rates, biomarker data are normalized to gram TOC.

Calculation of C/N weight ratios and determination of hydrogen indices were made in order to obtain first informations on the origin of the organic matter (terrigenous versus marine). In general, TOM shows C/N ratios >15, whereas MOM has low C/N ratios of ~5-7 [*Bordowskiy*, 1965; *Scheffer and Schachtschabel*, 1984]. However, it has to be taken into account that C/N ratios are also low in illite-enriched sediments because of significant amounts of inorganic nitrogen [*Müller*, 1977]. In immature carbon-rich (TOC >0.5%) sediments, HI <100 mg HC (g TOC)$^{-1}$ are typical for TOM, whereas organic matter with significant amounts of marine components has HI values of 200-400 mg HC (g TOC)$^{-1}$ [e.g., *Tissot and Welte*, 1984; *Stein*, 1991]. Downcore variations of C/N ratios and HI values indicate a clear dominance of TOM. C/N values vary between 10 and 20, whereas the hydrogen indices are lower than 100 mg HC (g TOC)$^{-1}$ throughout most of the core (Figure 3). Lower C/N ratios during OIS 1 and early OIS 2 are caused by high amounts of inorganic nitrogen (J. Knies, unpublished data, 1998). The $\delta^{13}C_{org}$ values vary between -24‰ and -27‰ during OIS 3, OIS 2, and Termination I and are widely regarded as an indicator of TOM in the Arctic Ocean (Figure 3) [*Ruttenberg and Göni*, 1997].

Selected types of biomarkers are used to assess in detail whether the organic matter is of land or marine origin. Long- ($C_{27}$, $C_{29}$ and $C_{31}$) and short-chain ($C_{17}$ and $C_{19}$) *n*-alkanes indicate the contribution of land-derived vascular plant material and the input of autochthonous MOM, respectively [e.g., *Eglinton and Hamilton*, 1963; *Gelpi et al.*, 1970; *Blumer et al.*, 1971; *Youngblood and Blumer*, 1973]. The concentration of long-chain *n*-alkanes ranges from 50 to 350 μg (g TOC)$^{-1}$ with no particular glacial/interglacial trend. The short-chain to long-chain *n*-alkane ratio ($C_{17,19}/C_{27,29,31}$) shows a predominance of TOM during early and late OIS 2, Termination I, and the Holocene (Figure 4). A distinct enrichment of long-chain *n*-alkanes is observed only during middle OIS 2 and Termination I.

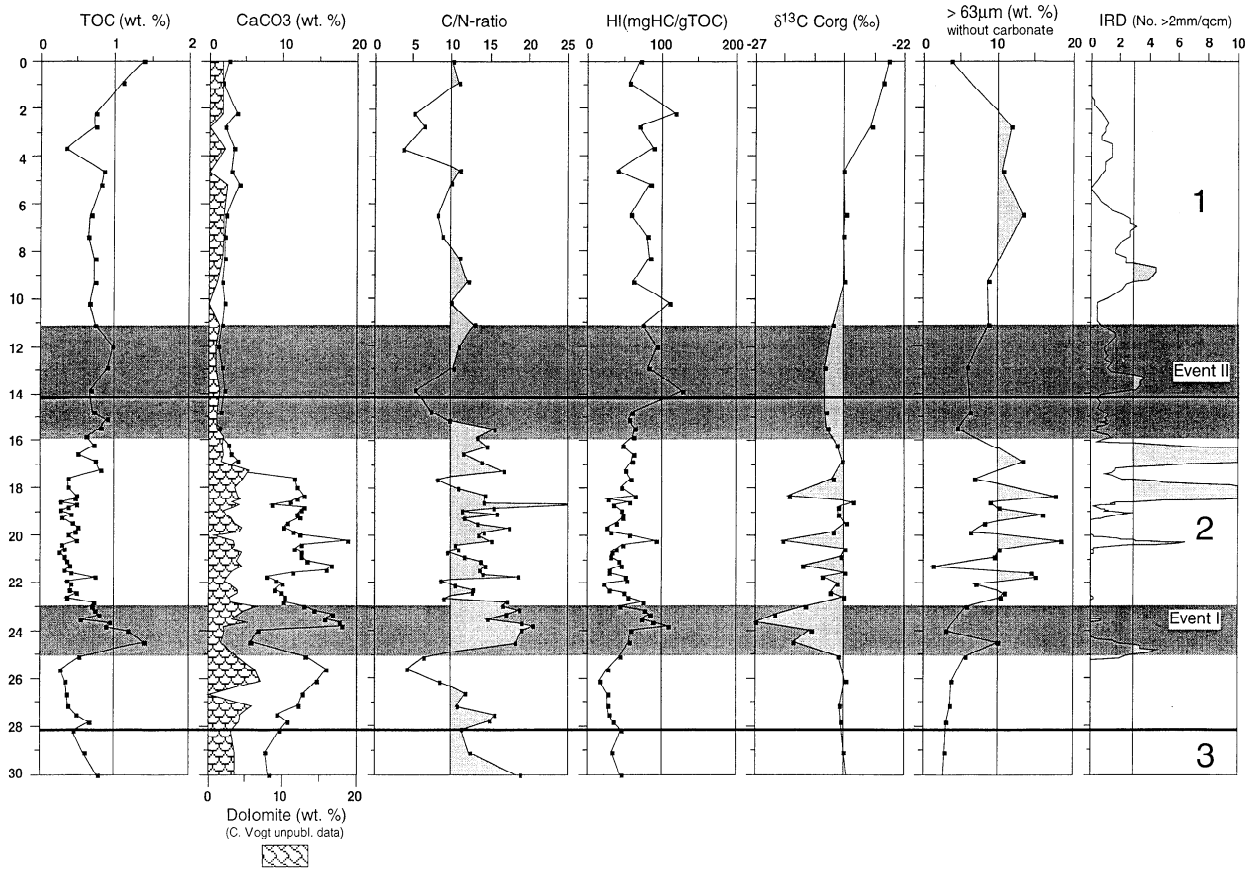


**Figure 3.** Total organic carbon, carbonate and dolomite content (all wt. %), C/N ratio, hydrogen index (HI)$\delta^{13}$ $C_{org}$ (per mill versus Vienna Pee Dee Belemnite), >63 µm fraction (wt. %), and ice-rafted debris (IRD) (>2 mm) data versus calibrated age.

As a good indicator of iceberg or sea ice transport, we used the records of IRD (>2 mm) and the coarse fraction (>63 µm) [*Hebbeln and Wefer*, 1997]. Continuous IRD input occurs primarily during Termination I and the Holocene. Short events in OIS 2 correlate well with increased input of coarse fraction and light $\delta^{13}C_{org}$ values (Figure 3). A distinct drop in IRD is observed in near-surface sediments. Higher input of detrital dolomite (up to 6%) is generally observed in glacial sediments during OIS 2 (Figure 3).

### 3.3. Marine Signal

In the Fram Strait and along the western Svalbard margin, calcite is well correlated to high numbers of planktonic and benthonic foraminifera [*Hebbeln and Wefer*, 1997]. The highest calcite concentrations (up to 12%) occur in late OIS 3 and during OIS 2, whereas OIS 1 is almost barren of foraminifera (Figure 3). A slight increase in MOM indicated by heavier $\delta^{13}C_{org}$ values (up to -22.5‰) occurs during the Holocene. Short-chain *n*-alkane concentration varies between 25 and 300 µg (g TOC)$^{-1}$ with a distinct maximum during middle OIS 2. Short- to long-chain *n*-alkane ratios >1 are also found during middle OIS 2, which is consistent with high chlorin concentrations and the abundances of $C_{37}$ alkenones and indicate a distinct higher input of MOM. Another peak of total chlorin, biogenic opal, and fatty acid (sum of 16:0, 16:1, and 18:1) concentrations and $C_{37}$ alkenones are observed during Termination I. The abundance of chlorins as a diagenetic product of chlorophyll has been related to primary productivity/preservation of autochthonous marine phytoplankton in sedimentary records [e.g., *Rosell-Melé and Koç*, 1997]. Additionally, in surface samples those fatty acids are described in algal material [cf. *Kates and Volcani*, 1966; *Fahl and Stein*, 1997, and references therein], although a contribution from bacterial or terrestrial input can not be excluded [c.f. *Boon et al.*, 1975; *Prahl et al.*, 1989]. Furthermore, long-chain unsaturated $C_{37}$-alkenones synthesized by haptophytes are used as a marine source indicator [e.g., *Volkman et al.*, 1980].

## 4. Discussion

### 4.1. Processes Controlling Deposition of MOM in the North Atlantic-Arctic Gateways: OIS 2

Regarding paleoceanographic reconstructions in the North Atlantic-Arctic Gateways region, meridional circulation patterns with seasonal or permanent Atlantic

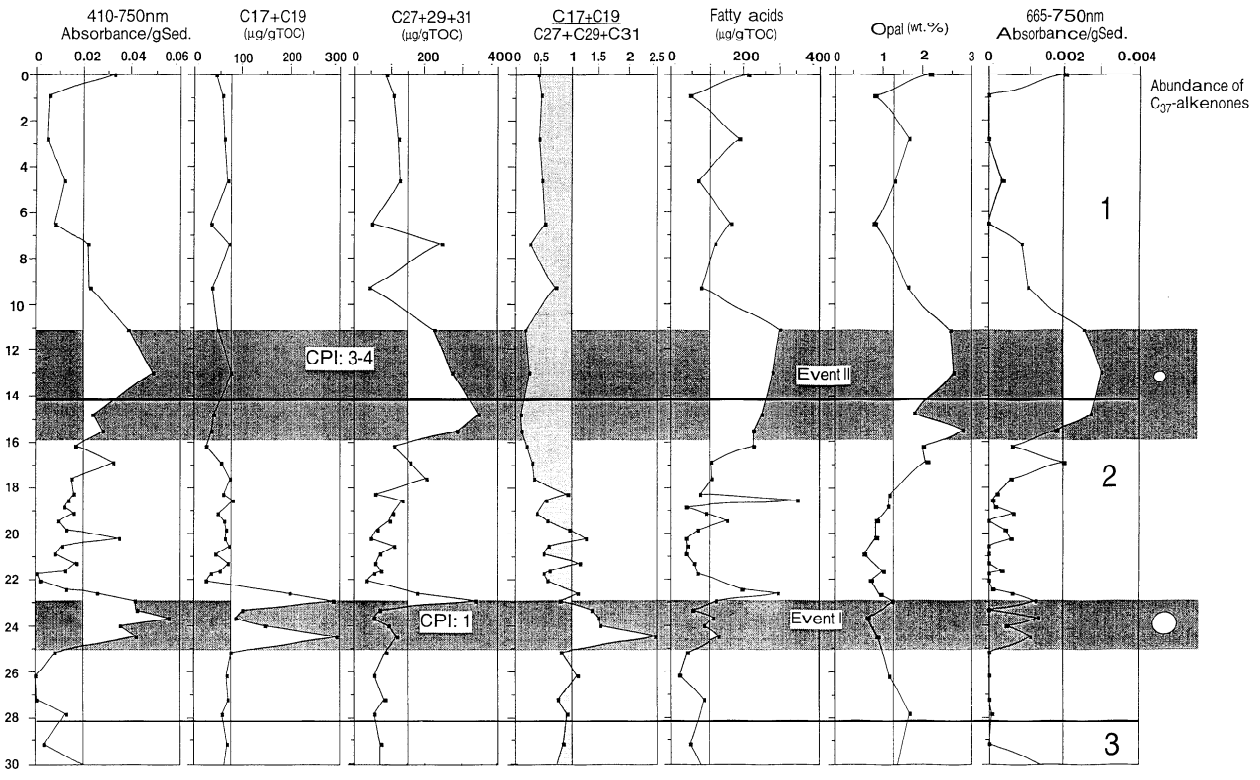


**Figure 4.** Compilation of total abundances of chlorophyll-derived pigments (410-750 nm (g sediment$^{-1}$), short- (marine-derived) and long-chain (terrigenous-derived) *n*-alkanes (µg (gTOC$^{-1}$)), ratio of marine- and terrigenous-derived*n*-alkanes, fatty acids (sum of 16:0, 16:1 (*n*-5) (*n*-7), 18:1 (*n*-7) (*n*-9) (µg (gTOC$^{-1}$)), opal content (wt. %), and chlorin-like pigments (665-750 nm g sediment$^{-1}$)) versus calibrated age. Abundances of $C_{37}$ alkenones are indicated as relative abundances of the total extract. It should be noted that alkenones could not be quantified in the sediment core. Low concentrations of $C_{37}$ alkenones were measured in two samples. Carbon Preference Index $(CPI)_{(21-32)}$ is reported according to *Bray and Evans* [1961]. Fresh terrigenous organic material has a CPI of 3-10, whereas that of fossil material varies ~1 [e.g., *Hollerbach*, 1985].

water advection have been reported during the last glacial/interglacial cycle [e.g., *Hebbeln et al.* 1994]. Two short time periods between 31.4-26.5 and 23-17.4 ka (27-22.5 and 19.5-14.5 $^{14}C$ ka) of relatively warm water advections from the North Atlantic into the Norwegian/Greenland Sea (NGS) served as a regional moisture source for the Svalbard/Barents Sea ice sheet (SBIS) build-up during the late Weichselian [*Hebbeln et al.*, 1994]. These periods are associated with increased abundances of coccoliths and subpolar planktonic and benthonic foraminifera [*Hebbeln and Wefer*, 1997] and are designated as high productive zones (HP) [*Dokken and Hald*, 1996]. Significant changes in composition and amount of MOM during these time intervals do not occur. Between 26.5 and 23 ka (22.5 and 19.5 $^{14}C$ ka) an intensified input of TOM is observed on the western Svalbard margin [*Hebbeln et al.*, 1994; *Elverhøi et al.*, 1995], which may indicate the first significant ice advance beyond the present coastline. In contrast, *Dokken* [1995] argued that this input reflects instead a deglaciation signal in between two periods of glacier growth within the late Weichselian. A distinct layer of coarse-grained material overlaid by laminated sediments between the high productive zones in core 2138 (Figure 2) supports this conclusion.

In general, the idea is that the input of these TOM-rich materials by retreating glaciers between 26.5 and 23 ka might be transported by dense bottom water currents from the shelf through the westward dipping troughs of the Svalbard margin into the eastern NGS. Feeding into intermediate Atlantic water masses, the material can be traced along the entire Barents Sea margin to the north and east [*Hebbeln et al.*, 1994; *Elverhøi et al.*, 1995; *Andersen et al.*, 1996]. Contemporaneous events with an input of reworked organic-rich material are recorded along the eastern Greenland margin [*Nam et al.*, 1995] from the northern Iceland Plateau and the Vøring Plateau [*Wagner and Henrich*, 1994].

High input of reworked TOM indicated by high C/N ratios (up to 20) and light $\delta^{13}C_{org}$ values (down to -27‰) between two high productive zones (HP1 and HP 2) (calcite content: up to 12 %) during the late Weichselian is also observed in PS2138-1 (Figure 3) and suggests similar paleoceanograhic conditions as described in the Fram Strait and at the western Svalbard margin [*Hebbeln et al.*, 1994; *Elverhøi et al.*, 1995; *Dokken and Hald*, 1996; *Hebbeln and Wefer*, 1997; *Knies et al.*, 1998]. The origin of the TOM-rich material could be related to sediments of the Spitsbergenbanken and the central Barents Sea [*Björlykke et al.*, 1978; *Elverhøi et al.*, 1995]. Organo geochemical studies

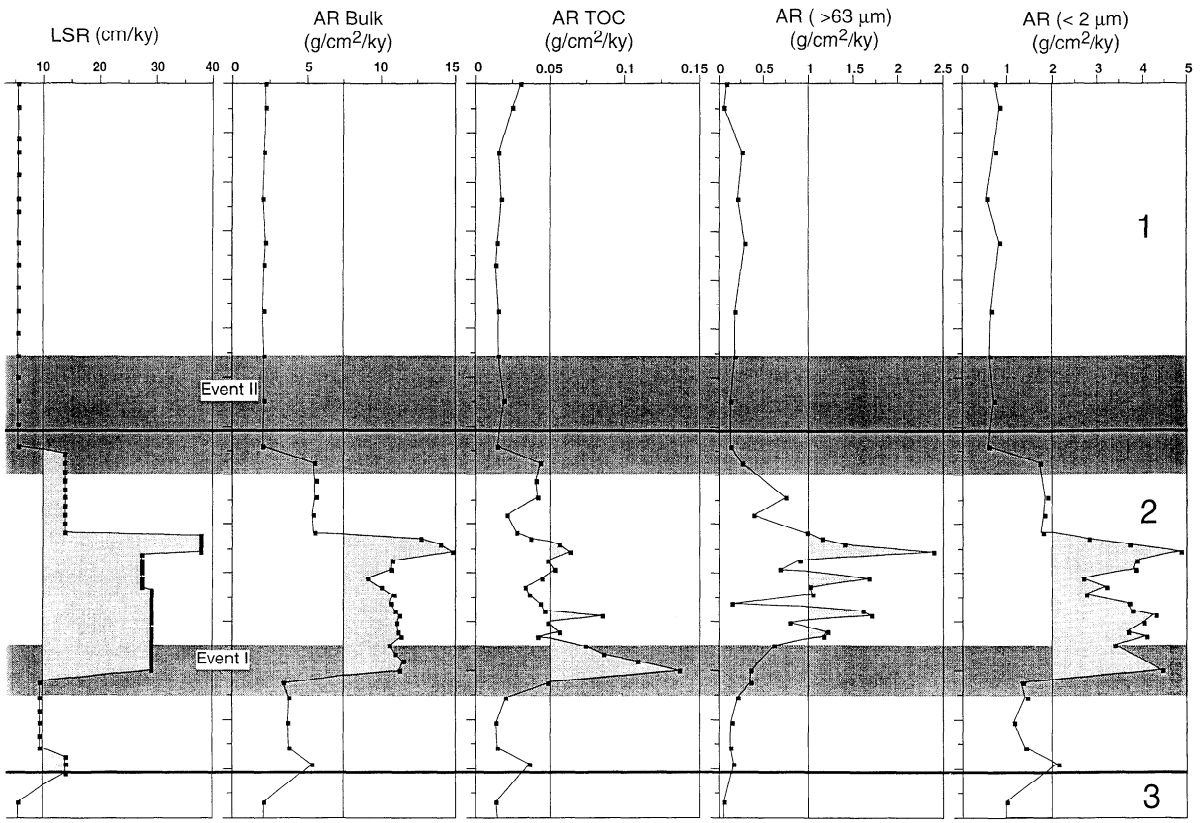


**Figure 5.** Linear sedimentation rate (cm $kyr^{-1}$) bulk mass accumulation rate (g $cm^{-2}$ $kyr^{-1}$), accumulation rates of organic carbon, the >63 µm fraction (without carbonate), and the <2 µm fraction (all in g $cm^{-2}$ $kyr^{-1}$) versus calibrated age.

of this material indicate that a reworked marine-derived source can be excluded. High C/N ratios (24), low hydrogen indices (70 mg HC (g TOC)$^{-1}$), and low oxygen indices (10 mg $CO_2$ (g TOC)$^{-1}$), and a high maturity ($T_{max}$: 470°C) confirm a reworked terrigenous source. In the remainder of the paper this time interval between 25 and 23 ka is described as Event I.

However, during the high productive zones, various indicative parameters demonstrate that the sedimentary organic matter is also predominantly of terrigenous origin: C/N ratios are mostly higher than 12, and HI values are lower than 100 mg HC (g TOC)$^{-1}$. Lighter $\delta^{13}C_{org}$ values are well correlated with distinct input of coarse- and fine-grained IRD (Figure 3). This TOM most probably originated in the Mesozoic strata cropping out along the western Scandinavian and Svalbard/Barents Sea shelf and was transported by glacial erosion to the deep sea [e.g., *Elverhøi et al.*, 1995; *Andersen et al.*, 1996; *Wagner and Henrich*, 1994; *Wagner and Hölemann*, 1995]. Increased accumulation rates of organic carbon (up to 0.45 g $cm^{-2}$ $kyr^{-1}$) during OIS 2 indicate an even higher absolute supply of TOM (Figure 5). However, a more detailed look at the marine- and terrigenous-derived biomarkers indicates that higher accumulation rates of MOM occur only during Event I. Despite the predominance of TOM during OIS 2 the ratio of short- to long-chain *n*-alkanes is generally >1 during Event I, which indicates a significant marine contribution. An enhanced marine influence is also documented by slightly increased fatty acid concentrations and abundances of long-chain unsaturated $C_{37}$ alkenones (Figure 4). The enhanced total absorbance of chlorophyll-derived pigments in this time interval cannot be easily related to MOM or TOM. However, a relative enrichment of chlorin-like pigments also reflects a slightly higher amount of MOM (Figure 4). The inconsistency of these results may be explained by a paleoenvironmental model shown in Figure 6.

The input of the organic-rich debris from the Spitsbergenbanken by retreating glaciers during Event I probably explains the enrichment of MOM in the underlying sediments. *Ittekkot et al.* [1992] described a similar process in the Arabian Sea, where increased vertical or lateral flux of fine-grained suspended material produces a scavenging and a higher adsorbance of autochthonous organic matter in the water column. *Deuser et al.* [1981] observed that an increase in total mineral flux is accompanied by an increase in MOM flux. Considering the average surface-water productivity during OIS 2, we assume that during the entire period, export production was more or less constant. However, owing to an increase of total flux of fine-grained (11 g $cm^{-2}$ $kyr^{-1}$) rather than coarse-grained (1 g $cm^{-2}$ $kyr^{-1}$) reworked TOM-rich material and high $AR_{bulk}$ (40 g $cm^{-2}$ $kyr^{-1}$), a better preservation of MOM is achieved (Figure 5) [*Müller and*

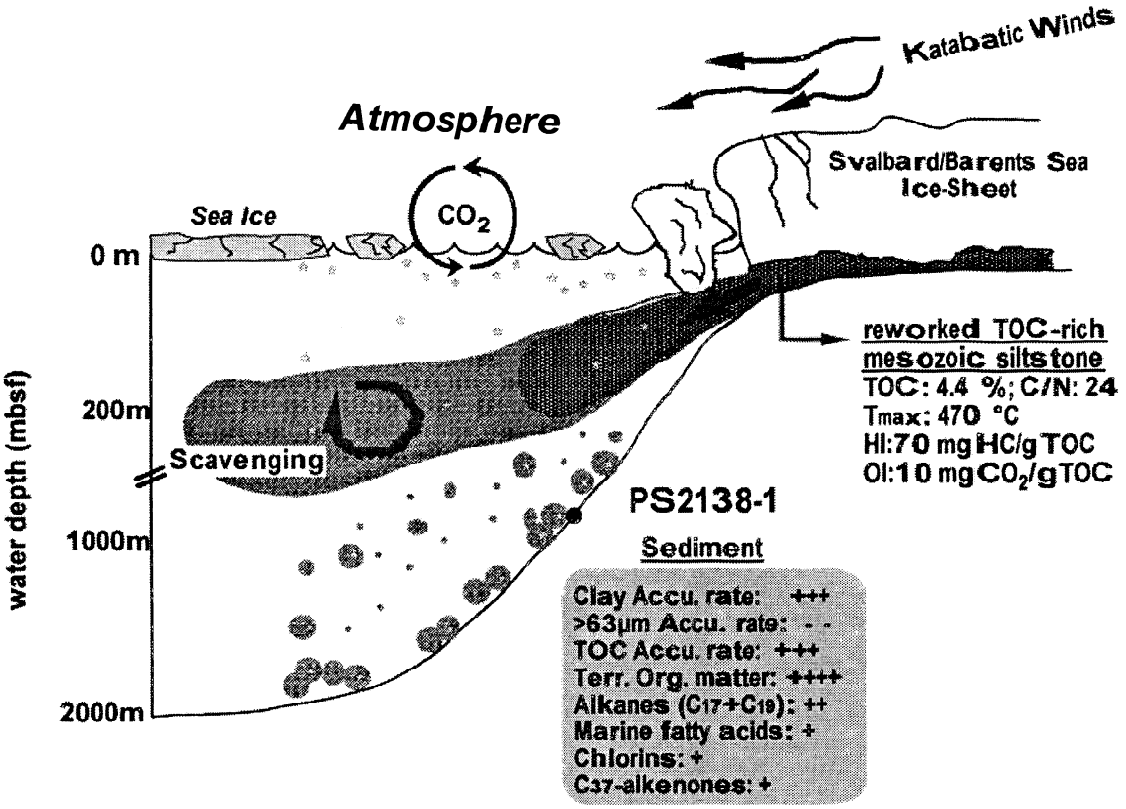


**Figure 6.** Model showing possible paleoenvironment along the northern Barents Sea margin during Event I. Reworked TOM-rich material transported by glaciers was picked out of the fraction >63 µm. Total organic carbon and nitrogen were measured by the CHN-elemental analyzer and HI and oxygen index (OI) by Rock Eval pyrolysis. Information regarding the maturity of the organic material can be obtained from the temperature of maximum pyrolysis yield $T_{max}$ [*Tissot and Welte*, 1984]. Climate-related sedimentary proxies in the sediment are listed in the shaded box.

*Suess*, 1979]. Thus the removal of MOM from the euphotic zone to the sediments is increased because of a rapid incorporation into fine-grained organic-rich mineral matter of terrigenous origin. The continuous flux of turbid meltwater suspensions at the grounding line of the glaciers support this process. Therefore respiration and decay of MOM are restricted in the water column. In contrast, input of coarser TOM and high sedimentation rates (up to 30 cm $kyr^{-1}$) during OIS 2 do not significantly influence the preservation of MOM (Figure 5).

This interpretation confirms partly a paleoenvironmental model by *Wagner and Hölemann* [1995]. This model describes an enhanced coupling of lithogenic and marine organic particles for periods of diamicton deposition in the NGS. They suggest that a better preservation of MOM is not related to enhanced export productivity or intensified inflow of relatively warm Atlantic water but to a more efficient vertical transport of MOM to the seafloor. In our case, we believe that the release of fine-grained and TOM-rich material by retreating ice sheets and associated high sedimentation rates (Figure 5) caused a more rapid transfer of MOM into the deep-water sphere by forming large aggregates of marine and terrigenous particles than an increased input of coarse-grained material and high sedimentation rates would have. Therefore we assume that despite this terrigenous organic background signal and assumed lower surface-water productivity during OIS 2 than that of the modern NGS, higher amounts of MOM were preserved during Event I rather than during the Holocene (with a stronger advection of Atlantic water) or at present [*Stein et al.*, 1994b; *Schubert and Stein*, 1996]. Although *Wheeler et al.* [1996] measured higher primary productivity rates in the water column of the central Arctic Ocean than previously expected, the benthonic respiratory demand and well-oxygenated bottom waters result in a very low accumulation rate of MOM in surface sediments [*Stein et al.*, 1994a, b; *Fahl and Stein*, 1997; *Boetius and Damm*, 1998]. Hence we conclude that the processes described during Event I and contemperaneous events in the NGS between 25 and 23 ka [*Wagner and Henrich*, 1994; *Nam et al.*, 1995; *Elverhøi et al.*, 1995] are more important for removal and preservation of autochthonous MOM in the Arctic Ocean and adjacent seas than are surface-water productivity changes (see discussion in, for example, *Emerson et al.*[1985]; *Pedersen and Calvert* [1990]).

### 4.2. Termination I

At the beginning of the last glacial-interglacial transition a rapid $\delta^{18}O$ depletion and a contemporaneous $\delta^{13}C$ minimum were recorded in the eastern Arctic Ocean at 18.6 ka (–15.7 $^{14}C$ ka) and at the Svalbard margin at 17.7 ka (–14.8 $^{14}C$ ka) [*Jones and Keigwin*, 1988; *Hebbeln et al.*, 1994; *Stein et al.*, 1994a]. These signals combined with a major contribution of IRD are interpreted as a major meltwater

anomaly, which probably reflects the onset of the decay of the SBIS in the southwestern Barents Sea and the western Svalbard margin [e.g., *Elverhøi et al.*, 1995]. At the northern Barents Sea margin the first distinct signal of ice recession is marked by a small but significant input of IRD at 19.1 ka. This is consistent with a first distinct deglacial signals around 18.9 ka (–16 $^{14}$C ka) at the southwestern Barents Sea margin proposed by *Vorren et al.* [1988]. A maximum pulse of IRD input at 18.3 ka may indicate the beginning retreat of the ice sheet from the shelf break (Figure 3). A second pulse of deglaciation is indicated by a distinct meltwater event ($\delta^{18}O$, 3.2‰; $\delta^{13}C$, -0.57‰) and IRD input before 14.8 ka. *Lubinski et al.* [1996] suggests that the northern Barents Sea margin at water depth ≥470 m was deglaciated at 15.2 ka (–13 $^{14}$C ka). Foraminiferal assemblages suggest that Atlantic-derived intermediate water may have begun to penetrate the Franz Victoria Trough on the northern Barents Sea margin 15.2 ka (–13 $^{14}$C ka) ago [*Lubinski et al.*, 1996]. This date is consistent with a permanent intrusion of Atantic water to the NGS and along the western Svalbard margin [*Hald and Vorren*, 1987; *Dokken*, 1995; *Sarnthein et al.*, 1995; *Hald and Aspeli*, 1997]. The retreat of the SBIS to the present shoreline was probably complete by 11.2 ka (10 $^{14}$C ka), which is supported by terrestrial evidence from Franz Josef Land and eastern Svalbard [*Forman et al.*, 1995, and references therein]. In the remainder of this paper the transition to postglacial marine sedimentation between 15.9 and 11.2 ka (13.5 and 10.0 $^{14}$C ka) on the northern Barents Sea margin is described as Event II.

Biogenic calcite is often used as the surface-water productivity indicator in the North Atlantic but is probably of limited value in analyzing Event II [e.g., *Hebbeln and Wefer*, 1997] since the carbonate content (3%-5%) is mainly composed of detrital dolomite instead of biogenic calcite (Figure 3). However, hydrogen indices exceeding 100 mg HC (g TOC)$^{-1}$ reflect the presence of slightly more MOM and stronger advection of Atlantic water during Event II. However, a predominant terrigenous source of the organic matter is documented by light $\delta^{13}C_{org}$ values (-25‰) (Figure 3). A closer look at the organic matter composition during Event II indicates that high concentrations of TOM and MOM were deposited (Figure 4). In particular, long-chain *n*-alkanes, total tetrapyrroles, biogenic opal, chlorin-like pigments, and fatty acids reach maximum values. In contrast to Event I the TOM appears to be dominantly "fresh" material indicated by carbon preferences indeces (CPI) >4 (Figure 4).

A possibility for better preservation of MOM during Event II could be a combination of higher nutrient supply, increasing phytoplankton growth, and an increased vertical flux of mineral and TOM-rich suspensions. In particular, melting of sea ice in the vicinity of the incipient warm Atlantic water intrusion provides large amounts of mineral suspensions and significantly increased surface-water productivity by the higher nutrients supply in the euphotic zone [*Nelson et al.*, 1989; *Fahl and Stein*, 1997]. Because of mineral adsorption of organic particles, larger aggregates stabilize the MOM, slowing remineralization rates and effecting a rapid removal into the deepwater sphere. A possible source for fresh TOM-rich material is the Laptev and Kara Sea shelf region [*Stein et al.*, 1994b; *Schubert and Stein*, 1997]. TOM on the shelf was eroded because of a rise in sea level transported by the Transpolar Drift and released because of intensive sea ice melting in the study area. Thus, labile MOM that was accumulated in the Arctic Ocean and its adjacent seas during Event II is optimally preserved because of increased primary production at the MIZ, higher settling flux of MOM, and sorptive protection by the high input of detrital and terrigenous organic material [e.g., *Calvert*, 1987; *Mayer*, 1994; *Keil et al.*, 1994]. In summary, preservation of autoch-thonous MOM in Arctic Ocean deposits is, in particular, linked to the lateral flux and deposition of mineral or TOM-rich ballast.

## 5. Conclusions

1. Generally, fluxes and variations of organic carbon composition in a sediment core on the northern Barents Sea margin do not reflect changes in paleo-surface-water productivity.

2. The removal of biologically fixed $CO_2$ into the deepwater sphere was increased between 25 and 23 kyr (Event I) because of a rapid incorporation into fine-grained mineral matter and a subsequent rapid transfer to the deep sea. In particular, the enhanced total flux of glacially eroded and fine-grained reworked TOM-rich material by retreating glaciers caused a better preservation of MOM due to a scavenging in the water column.

3. These "mineral ballast effects" are presumably seen in the NGS and are probably more important for preservation of MOM than are surface-water productivity changes.

4. The highest concentration of MOM was accumulated between 15.9 and 11.2 kyr (Event II) because of sorptive protection by detrital and terrigenous organic-rich material, high-suspension load and nutrient supply due to melting sea ice, and a permanent intrusion of relatively warm Atlantic water.

**Acknowledgments.** We thank the captain and the crew of the R/V *Polarstern* for cooperation during the ARKVIII/2-expedition. For discussion and reviews we thank B. Dieckmann, A. Mackensen, J. Matthiesen, C. Schubert, C. Vogt, and three anonymous reviewers. We thank K. Fahl for GC/MS operations. M. Siebold, G. Meyer, G. Traue, L. Schönicke, and P. Grootes are greatly acknowledged for laboratory and mass spectrometer operations. This is contribution 1348 of the Alfred Wegener Institute for Polar and Marine Research.

We are grateful to M. Delaney and P. Cooper for supporting publication.

## References

Andersen, E.S., T.M. Dokken, A. Elverhøi, A. Solheim, and I. Fossen, Late Quaternary sedimentation and glacial history of the western margin of Svalbard, *Mar. Geol., 133*, 123-156, 1996.

Anderson, L.G., Chemical oceanography of the Arctic and its shelf seas, in *Arctic Oceanography: Marginal Ice Zones and Continental Shelves*, Coastal and Estuarine Stud., vol. 49, edited by W. O. Smith and J.M. Grebmeier, pp. 183-202, AGU, Washington, D.C., 1995.

Anderson, L.G., and E.P. Jones, The transport of $CO_2$ into Arctic and Antarctic Seas: Similarities and differences in the driving processes, *J. Mar. Syst., 2*, 81-95, 1991.

**Bard, E., M. Arnold, and B. Hamelin, Presen**

status of the radiocarbon calibration of the late Pleistocene, paper presented at the 4th International Conference on Paleoceanography, Res. Cent. for Mar. Geosci., Kiel, Germany, 1992.

Bard, E., M. Arnold, R.G. Fairbanks, and B. Hamelin, $^{230}Th$-$^{234}U$ and $^{14}C$ ages obtained by mass spectrometry on corals, *Radiocarbon, 35*, 191-199, 1993.

Bjørlykke K., B. Bue, and A. Elverhøi, Quaternary sediments in the northwestern part of the Barents Sea and their relation to the underlying Mesozoic bedrock, *Sedimentology, 25*, 227-246, 1978.

Blindheim, J., Cascading of Barents Sea bottom water into the Norwegian Sea, *Rapp. P. V. Reun. Cons. Int. Explor. Mer., 188*, 49-58, 1989.

Blumer, M., R.R.L. Guillard, and T. Chase, Hydrocarbons of marine phytoplankton, *Mar. Biol., 8*, 183-189, 1971.

Boetius, A., and E. Damm, Benthic oxygen uptake, hydrolytic potentials and microbial biomass at the Arctic continental slope, *Deep Sea Res.*, 1998, in press, 1998.

Bonn, W., Biogenic opal and barium: Indicators for late Quaternary changes in productivity at the Antarctic continental margin, Atlantic Sector, *Rep. Polar Res., 180*, pp. 186, 1995.

Boon, J.J., J.W. de Leeuw, and P.A. Schenck, Organic geochemistry of Walvis Bay diatomaceous ooze, I, Occurence and significance of the fatty acids, *Geochim. Cosmochim. Acta, 39*, 1559-1565, 1975.

Bordowskiy, O.K., Sources of organic matter in marine basins, *Mar. Geol., 3*, 5-31, 1965.

Boyle, E.A., Vertical oceanic nutrient fractionation and glacial/interglacial $CO_2$ cycles, *Nature, 331*, 55-56, 1988.

Bray, E.E., and E.D. Evans, Distribution of *n*-paraffins as a clue to recognition of source beds, *Geochim Cosmochim. Acta, 22*, 2-15, 1961.

Broecker W., G. Bond, and M. Klas, A salt oscillator in the Glacial Atlantic, *Paleoceanography, 5*, 469-477, 1990.

Calvert, S.E., Oceanographic controls on the accumulation of organic matter in marine sediments, in *Marine Petroleum Source Rocks*, edited by J. Brooks and A. J. Fleet, pp. 137-151, Geol. Soc. London Spec. Publ., 1987.

Deuser, W.G., E.H. Ross, and R.F. Anderson, Sea-sonality in the supply of sediment to the deep Sargasso Sea and implications for the rapid transfer of matter to the deep ocean, *Deep Sea Res., Part A, 28*, 495-505, 1981.

Dokken, T.M., Paleoceanographic changes during the last interglacial-glacial cycle from the Svalbard-Barents Sea margin: Implications for ice-sheet growth and decay, PhD. thesis, 175 pp., Univ. of Bio. and Geol., Tromsø, Norway, 1995.

Dokken, T.M., and M. Hald, Rapid climatic shifts during isotope stages 2-4 in the Polar North Atlantic, *Geology , 24*, 599-602, 1996.

Eglinton, G., and R.J. Hamilton, The distributions of alkanes, in *Chemical Plant Taxonomy*, edited by T. Swain, pp. 187-217, Academic, San Diego, Calif., 1963.

Elverhøi A., E.S. Andersen, T.M. Dokken, R. Spielhagen, J.I. Svendsen, M. Sørflaten, A. Rørnes, M. Hald, and C.F. Forsberg, The growth and decay of the late Wechselian Ice Sheet in western Svalbard and adjacent areas based on provenance studies of marine sediments, *Quat. Res., 44*, 303-316, 1995.

Emerson, S., K. Fischer, C. Reimers, and D. Heggies, Organic carbon dynamics and preservation in deep sea sediments, *Deep Sea Res., Part A, 32*, 1-21, 1985.

Emmerman, R., and J. Lauterjung, Double X-ray analysis of cuttings and rock flour: A powerful tool for rapid and reliable determination of borehole lithostratigraphy, *Sci. Drill., 1*, 269-282, 1990.

Espitalié, J., J.L. Laporte, M. Madec, F. Marquis, P. Leplat, J. Paulet, and A. Boutefeu, Méthode rapide de chararcterisation des roches-mere de leur potential petrolier et de leur degre d'évolution, *Rev. Inst. Tr. Pet., 32*, 23-42, 1977.

Fahl, K., and R. Stein, Modern organic-carbon-deposition in the Laptev Sea and the adjacent continental slope: Surface-water productivity vs. terrigenous supply, *Org. Geochem., 26*, 379-390, 1997.

Forman, S.L., D. Lubinski, G.H. Miller, J. Snyder, G. Matishov, S. Korsun, and V. Myslivets, Postglacial emergence and distribution of late Weichselian ice-sheet loads in the northern Barents and Kara Seas, Russia, *Geology, 23*, 113-116, 1995.

Gealy, E.L., Saturated bulk density, grain density, and porosity of sediment cores from the western equatorial Pacific: Leg 7, Glomar Challenger, *Initial Rep. Deep Sea Drill. Proj., 7*, 1081-1104, 1971.

Gelpi, E., H. Schneider, J. Mann, and J. Oró, Hydrocarbons of geochemical significance in microscopic algae, *Phytochemistry, 9*, 603-612, 1970.

Grobe, H., A simple method for the determination of ice-rafted debris in sediment cores, *Polarforschung, 57*, 123-126, 1987.

Hald, M., and R. Aspeli, Rapid climatic shifts of the northern Norwegian Sea during the last deglaciation and the Holocene, *Boreas*, 26, 15-28, 1997.

Hald, M., and T. Vorren, Foraminiferal stratigraphy and environments of Late Weichselian deposits on the continental shelf off Troms, Northern Norway, *Marine Micropaleontology*, 12, 129-160, 1987.

Hebbeln, D., and G. Wefer, Late Quaternary paleoceanography in the Fram Strait, *Paleoceanography, 12*, 49-65, 1997.

Hebbeln D., T.M. Dokken, E.S. Andersen, M. Hald, and A. Elverhøi, Moisture supply for northern ice-sheet growth during the last glacial maximum, *Nature, 370*, 357-359, 1994.

Heimdal, B.R., Phytoplankton and nutrients in the waters north-west of Spitsbergen in the autumn of 1979, *J. Plankton Res., 5*, 901-918, 1983.

Hollerbach, A., Grundlagen der Organischen Geochemie, 190 pp., Springer-Verlag, New York, 1985.

Ittekkot, V., B. Haake, M. Bartsch, R.R. Nair, and V. Ramaswamy, Organic carbon removal in the sea: The continental connection, in *Uppwelling Systems: Evolution Since the Early Miocene*, edited by. C.P. Summerhayes, W.L. Prell, and K.C. Emeis, *Geol. Soc. Spec. Publ., 64*, 167-176, 1992.

Jones, G.A., and Keigwin, L.D., Evidence from Fram Strait (78°N) for early deglaciation, *Nature, 336*, 56-59, 1988.

Kates, K., and B.E. Volcani, Lipid components of diatoms, *Biochem. Biophys. Acta, 116*, 264-278, 1966.

Kattner, G., and H.S.G. Fricke, Simple gas-liquid chromatographic method for simultaneous determination of fatty acids and alcohols in wax esters of marine organisms, *J. Chromat., 361*, 313-318, 1986.

Keil, R.G., D.B. Montlucon, F.G. Prahl, and J.I. Hedges, Sorptive preservation of labile organic matter in marine sediments, *Nature, 370*, 549-551, 1994.

Knies, J., C. Vogt, and R. Stein, Late Quaternary growth and decay of the Svalbard-Barents Sea ice sheet and paleoceanographic evolution in the adjacent Arctic Ocean, *Geo. Mar. Lett.*, in press, 1998.

Lubinski, D.J., S. Korsun, L. Polyak, S.L. Forman, S.J. Lehman, F.A. Herlihy, and G.H. Miller, The last deglaciation of the Franz Victoria Trough, northern Barents Sea, *Boreas, 25*, 89-100, 1996.

Macdonald, R., Awakenings in the Arctic, *Nature, 380*, 286-287, 1996.

Mackensen, A., H. Grobe, H.-W. Hubberten, and G. Kuhn, Benthic foraminiferal assemblages from the eastern South Atlantic Polar Front region between 35° and 57°S: Glacial-to-interglacial contrasts, in *Carbon Cycling in the Glacial Ocean: Constraints on the Oceans' Role in Global Change*, NATO ASI Ser. I, vol. 17, edited by R. Zahn et al., 105-144, Springer-Verlag, New York, 1994.

Mangerud, J., and S. Gulliksen, Apparent radiocarbon ages of recent marine shells from Norway, Spitsbergen, Arctic Canada, *Quat. Res., 5*, 273-296, 1975.

Martinson, D.G., N.G. Pisias, J.D. Hays, J. Imbrie, T.C. Moore, and N.J. Shakleton, Age dating and the orbital theory of the Ice Ages: Development of a high-resolution 0 to 300,000 year chronostratigraphy, *Quat. Res., 27*, 1-27, 1987.

Mayer, L. M., Surface area control of organic carbon accumulation in continental shelf sediments, *Geochim. Cosmochim. Acta, 58*, 1271-1284, 1994.

Midttun, L., Formation of dense bottom water in the Barents Sea, *Deep Sea Res., Part A, 2*, 1233-1241, 1985.

Müller, G., *Methods in Sedimentary Petrology*, 283 pp., Schweizerbart, Stuttgart, 1967.

Müller, P., C/N ratios in Pacific deep-sea sediments: Effect of inorganic ammonium and organic nitrogen compounds sorbed by clays, *Geochim. Cosmochim. Acta, 41*, 765-776, 1977.

Müller, P., and R. Schneider, An automated leaching method for the determination of opal in sediments and particulate matter, *Deep-Sea Res., 40*, 425-444, 1993.

Müller, P., and E. Suess, Productivity, sedimentation rate, and sedimentary organic matter in the oceans, I, Organic matter preservation, *Deep Sea Res., 26*, 1347-1362, 1979.

Nam, S.I., R. Stein, H. Grobe, and H. Hubberten, Late Quaternary glacial-interglacial changes in sediment composition at the east Greenland continental margin and their paleoceanographic implications, *Mar. Geol., 122*, 243-262, 1995.

Nelson, D.M., W.O. Smith, R.D. Muench, L.I Gordon, C.W. Sullivan, and D.M. Husby, Particulate matter and nutrient distribution in the ice-edge zone of the Weddell Sea: Relationship to hydrogaphy during late summer, *Deep Sea Res., Part A, 36*, 191-209, 1989.

Pedersen, T.F., and S.E. Calvert, Anoxia vs. Productivity: What controls the formation of organic-carbon-rich sediments and

sedimentary rocks?, *AAPG Bull.*, *74*, 454-466, 1990.

Prahl, F.G., L.A. Muehlhausen, and M. Lyle, An organic geochemical assessment of oceanographic conditions at Manop Site C over the past 26,000 years, *Paleoceanography*, *4*, 495-510, 1989.

Quadfasel, D., B. Rudels, and K. Kurz, Outflow of dense water from a Svalbard fjord into the Fram Strait, *Deep Sea Res., Part A 35*, 1143-1150, 1988.

Rachor, E., (Ed.), Scientific cruise report of the 1991 Arctic expedition ARK VIII/2 of R/V *Polarstern* (EPOS II), *Rep. Polar Res.*, *115*, 149, 1992.

Rosell-Melé, A., and N. Koc, Paleoclimatic significance of the stratigraphic occurrence of photosynthetic biomarker pigments in the Nordic seas, *Geology*, *25*, 49-52, 1997.

Rosell-Melé, A., M.A. Maslin, J.R. Maxwell, and P. Schaeffer, Biomarker evidence for Heinrich events, *Geochim. Cosmochim. Acta*, *61*, 1671-1678, 1997.

Rudels, B., E.P. Jones, L.G. Anderson, and G. Kattner, On the intermediate depth waters of the Arctic Ocean, in *The Polar Oceans and Their Role in Shaping the Global Environment*, Geophys. Monogr. Ser., vol. 85, edited by O.M. Johannessen, R. Muench, and J. Overland, pp. 33-46, AGU, Washington D. C.,1994.

Ruttenberg, K.C., and M.A. Gõni, Phosphorus distribution, C:N:P ratios, and $\delta^{13}$Corg in arctic, temperate, and tropical coastal sediments: Tools for characterizing bulk organic matter, *Mar. Geol.*, *139*, 123-145, 1997.

Sarnthein, M., et al., Variations in Atlantic surface ocean paleoceanography, 50-80°N: A time-slice record of the last 30,000 years, *Paleoceanography*, *10*, 1063-1094, 1995.

Scheffer, F., and P. Schachtschabel, *Lehrbuch der Bodenkunde*, 442 pp.Enke-Verlag, Stuttgart, 1984.

Schubert, C.J., and R. Stein, Deposition of organic carbon in Arctic Ocean sediments: Terrigenous supply vs. marine productivity, *Org. Geochem.*, *24*, 421-436, 1996.

Schubert, C.J., and R. Stein, Lipid distribution in surface sediments from the eastern central Arctic Ocean, *Mar. Geol.*, *138*, 11-25, 1997.

Stein, R., Accumulation of organic carbon in marine sediments, in *Lecture Notes in Earth Science*, vol. 34, 217 pp., Springer-Verlag, New York, 1991.

Stein R., C. Schubert, C. Vogt, and D. Fütterer, Stable isotope stratigraphy, sedimentation rates, and salinity changes in the latest Pleistocene to Holocene eastern central Arctic Ocean, *Mar. Geol.*, *119*, 333-355, 1994a.

Stein R., H. Grobe, and M. Wahsner, Organic carbon, carbonate, and clay mineral distributions in eastern central Arctic Ocean surface sediments, *Mar. Geol.*, *119*, 269-285, 1994b.

Stuiver, M., and P.J. Reimer, Extended $^{14}$C data base and revised CALIB 3.0 $^{14}$C age calibration program, *Radiocarbon*, *35*, 215-230, 1993.

Sudgen, D.E., *Arctic and Antarctic: A Modern Geographical Synthesis*, publications, 472 pp., Blackwell,Cambridge, Mass., 1982.

Thiede, J., A.M. Myhre, J.V. Firth, G.L. Johnson, and W.F. Ruddiman (Eds.), *Proceedings of the Ocean Drilling Program Science Results*, vol. 151: College Station, Texas, 1996.

Tissot, B.P., and D.H. Welte, *Petroleum Formation and Occurence*, 699 pp., Springer-Verlag, New York, 1984.

Van Andel, T.H., G.R. Heath, and T.C. Moore, Cenozoic History and Paleoccanography of the Central Equatorial Pacific, *Mem. Geol. Soc. Am.*, *143*, 134, 1975.

Volkman, J.K., G. Eglinton, E.D.S. Corner, and T.E.V. Forsberg, Long-chain alkenes and alkenones in the marine coccolithophorid *Emiliania hyxleyi*, *Phytochemistry*, *19*, 2619-2622, 1980.

Vorren, T.O., M. Hald M, and E. Lebesbye, Late Cenozoic environment in the Barents Sea, *Paleoceanography*, *3*, 601-612, 1988.

Wagner, T., and R. Henrich, Organo- and lithofacies of glacial-interglacial deposits in the Norwegian-Greenland Sea: Responses to paleoceanographic and paleoclimatic changes, *Mar. Geol.*, *120*, 335-364, 1994.

Wagner, T., and J.A. Hölemann, Deposition of organic matter in the Norwegian-Greenland Sea during the past 2.7 million years, *Quat. Res.*, *44*, 355-366, 1995.

Wheeler, P.A., M. Gosselin, E. Sherr, D. Thibault, D.L. Kirchman, R. Benner, and T.E. Whitledge, Active cycling of organic carbon in the central Arctic Ocean, *Nature*, *380*, 697-699, 1996.

Youngblood, W.W., and M. Blumer, Alkanes and alkenes in marine benthic algae, *Mar. Biol.*, *21*, 163-172, 1973.

J. Knies and R. Stein, Alfred Wegener Institute for Polar and Marine Research, Columbusstrasse, 27568 Bremerhaven, Germany. (email: jknies@awi-bremerhaven.de)

(Received July 1, 1997;
revised December 29, 1997;
accepted May 1, 1998.)